SLAC–AP–125
July, 2000

Searching for Transverse Sawtooth in Strong Head-Tail Instability by Adding Landau Damping*

Boaz Nash and Alex Chao
Stanford Linear Accelerator Center, Stanford University, Stanford, CA 94309

1 Introduction

In an effort to explain transverse sawtooth patterns observed by BPM's in some electron storage rings, we consider a simple two-macroparticle model for beam dynamics,

$$\ddot{x}_1 + (\alpha + \alpha_1 I_1)\dot{x}_1 + \omega_\beta^2 x_1 = 0 \tag{1}$$

$$\ddot{x}_2 + (\alpha + \alpha_1 I_2)\dot{x}_2 + \omega_\beta^2 x_2 = W x_1 \tag{2}$$

where the roles of particle 1 and particle 2 are switched every time interval $T_s/2$. The $\alpha_1 I_i$ terms are to be thought of as a simple model of Landau damping imposed on the two-particle model, where we have

$$I_i = x_i^2 + \frac{\dot{x}_i^2}{\omega_\beta^2} \tag{3}$$

with i taking on values of 1 or 2.

*Work supported by Department of Energy contract DE–AC03–76SF00515.

2 Numerical Methods

The above equations were integrated numerically using a thin lens approximation impulse approach to be described later. The paramter values used were as follows. α was varied, a typical value being 1200 s^{-1}. A typical value for α_1 was $1 \times 10^9 m^{-2} s^{-1}$. T_s, the synchrotron period was 1.66×10^{-4} seconds. The betatron frequency ω_β was 1.564426×10^7 s^{-1}. The coupling between the two macroparticles was controlled by the paramater W which was computed by

$$W = \frac{N r_0 W_0 c^2}{2\gamma \bar{C}} \tag{4}$$

where N, the number of particles was typically 6.144×10^{11}, r_0, the classical electron radius is $2.818 \times 10^{-15} m$, W_0, the transverse wake function used was 5.8×10^5 m^{-2}, c, the speed of light is 3×10^8 m/s, the relativistic factor γ used was 28375.7, and the circumference of the ring $\bar{C}$ was 2200 m.

These values correspond to a value for W of $7.2387 \times 10^{11} s^{-2}$. The relevant unitless parameter determining the stability in the case $\alpha_1 = 0$ is

$$\Upsilon = \frac{W T_s}{4\omega_\beta} \tag{5}$$

and the above parameter values lead to a value of $\Upsilon/2 = 0.96$. For $\alpha_1 = 0$, the dynamics are unstable for $\Upsilon/2 > 1$. Υ can be varied by varying the number of particles, N.

In the absence of damping and coupling, the motion of each particle is sinusoidal. The damping and coupling were added as perturbations on the sinusoidal motion, the integrated effect applied as an impulse, changing the velocity of each particle at a time half-way through each small time increment dt. Let

$$\mathcal{M}(T) = \begin{pmatrix} \cos(\omega_\beta T) & \sin(\omega_\beta T) \\ -\sin(\omega_\beta T) & \cos(\omega_\beta T) \end{pmatrix} \tag{6}$$

and

$$\mathbf{x}_i = \begin{pmatrix} x_i \\ \dot{x}_i/\omega_\beta \end{pmatrix} \tag{7}$$

Then, given $x_i(t)$ and $\dot{x}_i(t)$, we compute:

$$\mathbf{x}_a = \mathcal{M}(dt/2)\mathbf{x}_i(t) \tag{8}$$

$$x_b = x_a \tag{9}$$

$$\dot{x}_b = \dot{x}_a + f(x_a, \dot{x}_a) * dt \tag{10}$$

$$x_b, \dot{x}_b \Rightarrow \mathbf{x}_b \tag{11}$$

$$\mathbf{x}_i(t+dt) = \mathcal{M}(dt/2)\mathbf{x}_b \tag{12}$$

For the front particle, x_1, we have

$$f(x, \dot{x}) = -(\alpha + \alpha_1 I_1)\dot{x} \tag{13}$$

whereas for the back particle, x_2, we have

$$f(x, \dot{x}) = -(\alpha + \alpha_1 I_2)\dot{x} + W x_1 \tag{14}$$

This procedure was iterated for $0 < t < T_f$ where T_f was typically around 0.01 sec with $dt = 10^{-9}$ sec. The center of mass $\bar{X} = \frac{x_1+x_2}{2}$ was computed at each iteration. Discrete Fourier transforms were computed of the time step data using a standard FFT.

3 Results

With $\alpha_1 = 0$, the stability of the motion is determined by Υ. $\bar{X}$ diverges exponentially for $\Upsilon/2 > 1$. By turning on α_1 a steady state bounded motion results. The center of mass motion is shown in figure 1. Figure 2 shows $x_1(t)$ (the head particle) and $x_2(t)$ (the tail particle). In the steady state, the amplitude of the head oscillations decay, first causing the tail oscillations to lose amplitude, then to gain amplitude until the amplitude of the tail oscillations reaches the original amplitude of the head oscillations. The switching of phase required to go from head oscillations decreasing the amplitude of tail oscillations to causing increasing amplitude of tail oscillations occurs at the minimum amplitude of tail oscillation.

With $\alpha_1 = 10^9 m^{-2} s^{-1}$, the α damping term is insignificant. Thus, we take $\alpha = 0$ in all that follows. Figure 3 shows the major peaks in the power spectra of the center of mass motion for $\Upsilon/2 = .9$ and 1.3. Figure 4 shows the whole spectrum, displaying the fact that no low frequency modulation occurs in this model.

The frequencies of the three largest peaks for varying values of Υ are shown in figure 5. The peaks are split by an amount close to twice the synchrotron frequency for small Υ converging to individual peaks as $\Upsilon/2 \rightarrow 1$. The locations of the peaks for $\Upsilon/2 < 1$ are the same with a high accuracy

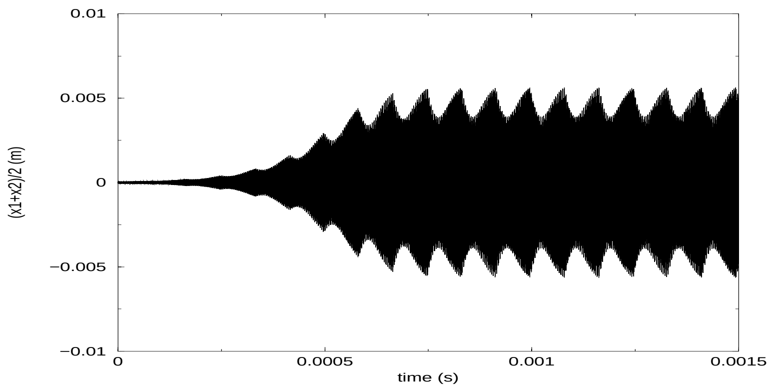

Figure 1: Center of mass motion for $\Upsilon/2 = 1.3$. $\alpha = 1200s^{-1}$, $\alpha_1 = 10^9 m^{-2}s^{-1}$.

with α_1 turned on or off. Because with $\alpha_1 = 0, \Upsilon/2 \geq 1$ the motion diverges, it makes sense to continue the plot only for $\alpha_1 > 0$; thus, the points in figure 5 with $\Upsilon/2 \geq 1$ represent spectra with $\alpha_1 = 10^9 m^{-2}s^{-1}$.

Finally, we note that if the data is strobed at the frequency of revolution, a saw-tooth like pattern emerges due to the sampling of the higher frequency betatron oscillations. This is possibly an artifact due to the simplicity of the two-particle model. The result of this strobing for $\Upsilon/2 = 1.3$ is shown in figure 6.

4 Conclusion

The addition of a non-linear damping term proportional to the macroparticle energy does indeed produce stability in the otherwise unstable $\Upsilon/2 > 1$ region. The stable motion shown in figure 1 involves betatron oscillations modulated by the synchrotron oscillations. No other lower frequency modulation is observed to occur, i.e. this model shows no evidence of a sawtooth behavior. If the motion is strobed at the revolution frequency, however, a slower sawtooth like modulation is observed, resulting from sampling effects of the higher frequency betatron and synchrotron oscillations.

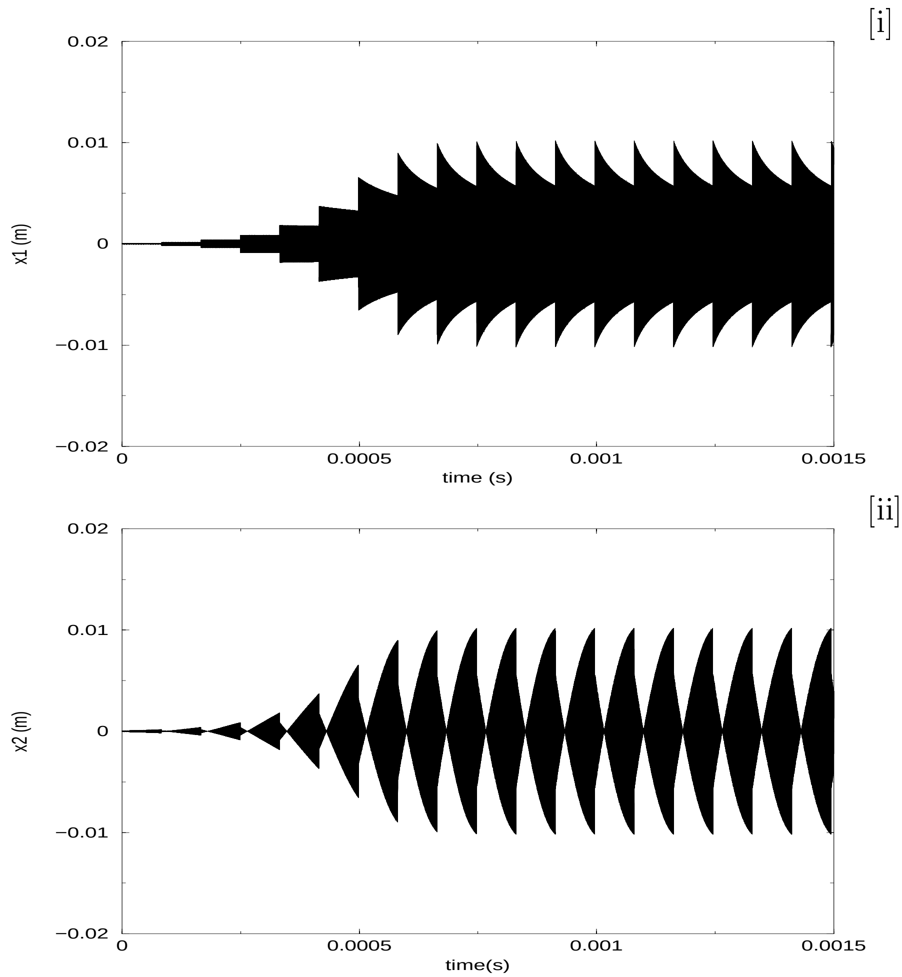

Figure 2: Head and tail oscillations: [i]$x_1(t)$ and [ii]$x_2(t)$. The paramaters used are the same as those in figure 1.

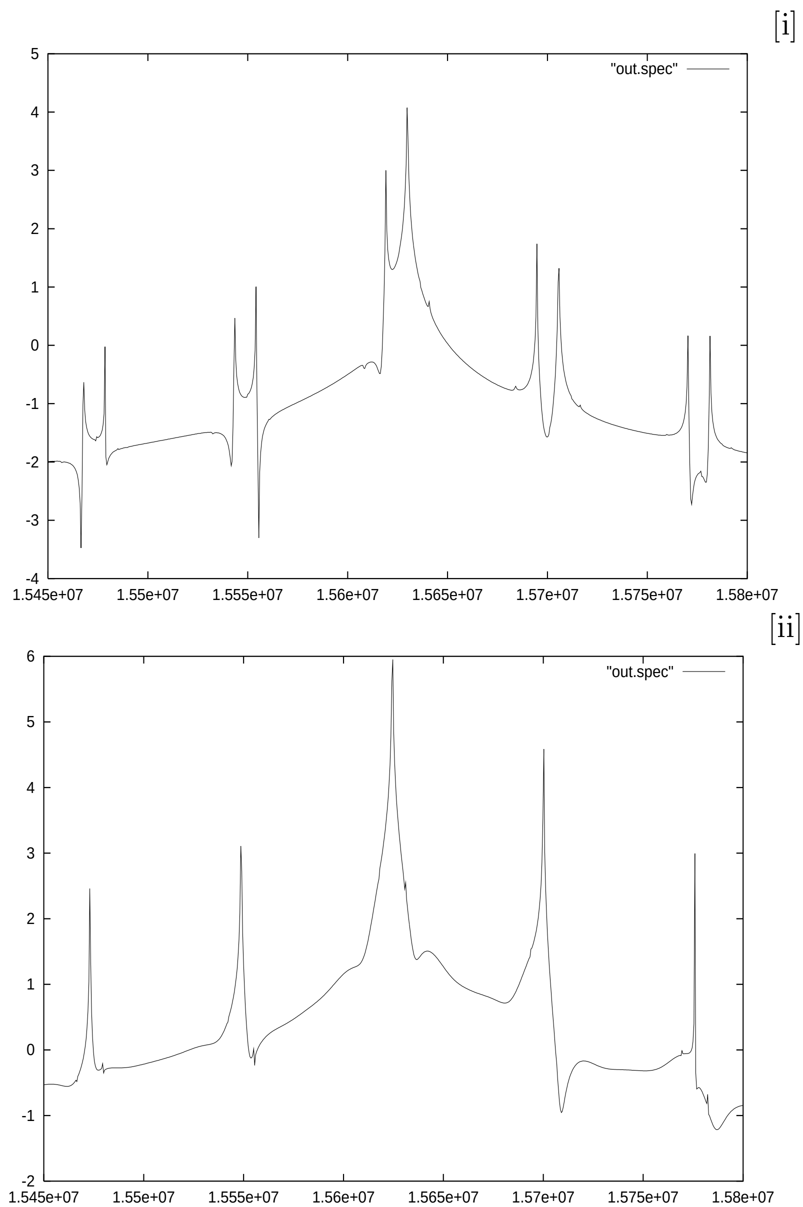

Figure 3: Log of power spectra of $\bar{X}$ for $\Upsilon/2 =$ [i] .9, [ii] 1.3.

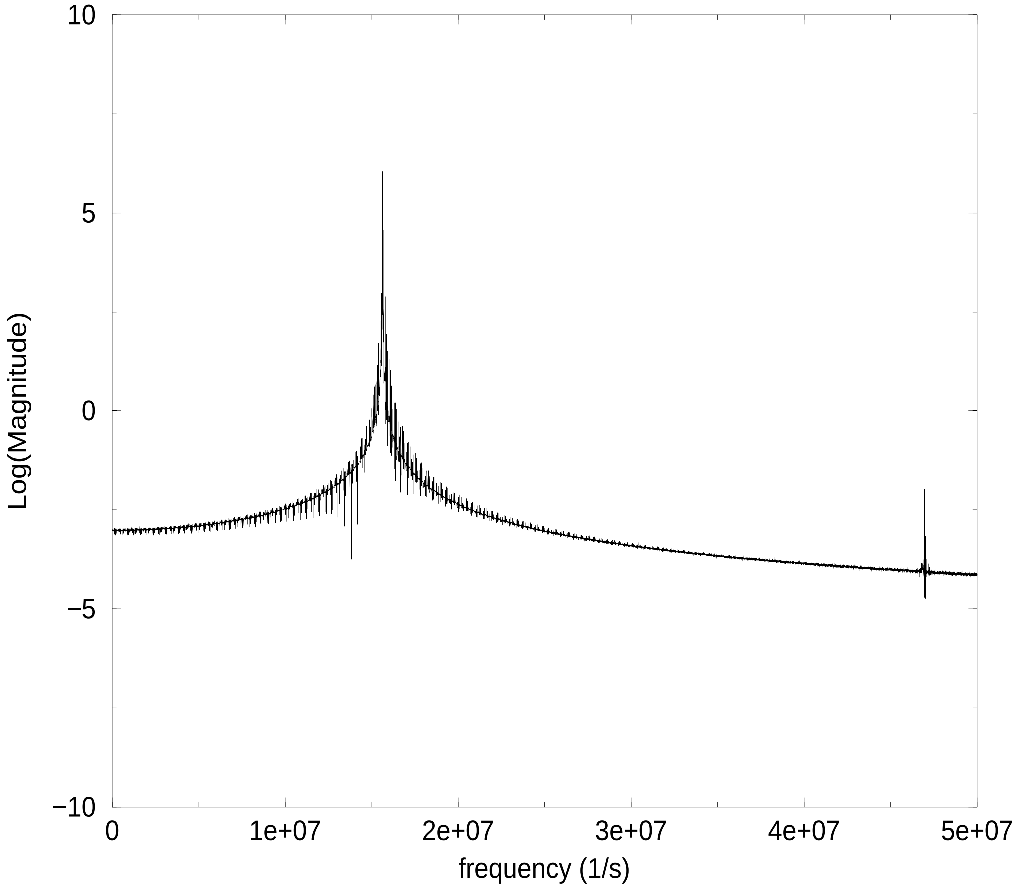

Figure 4: Power spectra of $\bar{X}$ for $\Upsilon/2$ =1.3.

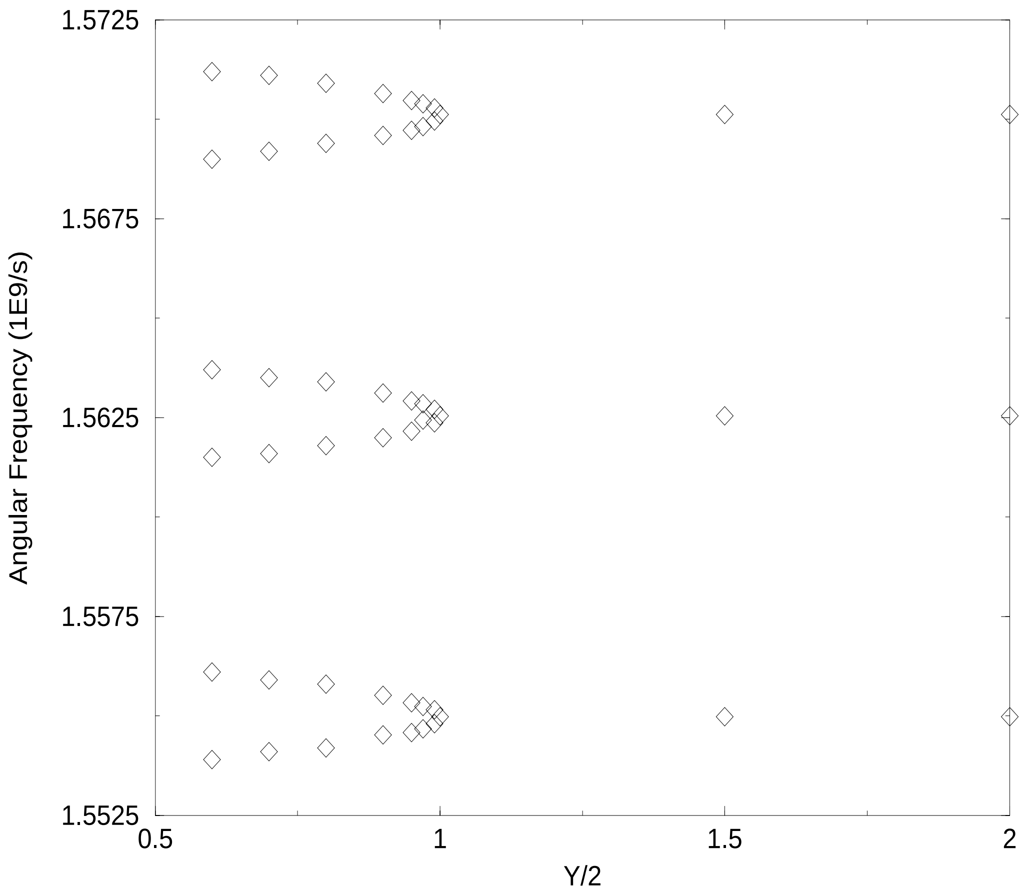

Figure 5: Distribution of peaks from Fourier Transform of $\bar{X}$. $\alpha = 0$, $\alpha_1 = 0$ for $\Upsilon/2 < 1$ and $\alpha_1 = 10^9 m^{-2} s^{-1}$ for $\Upsilon/2 \geq 1$.

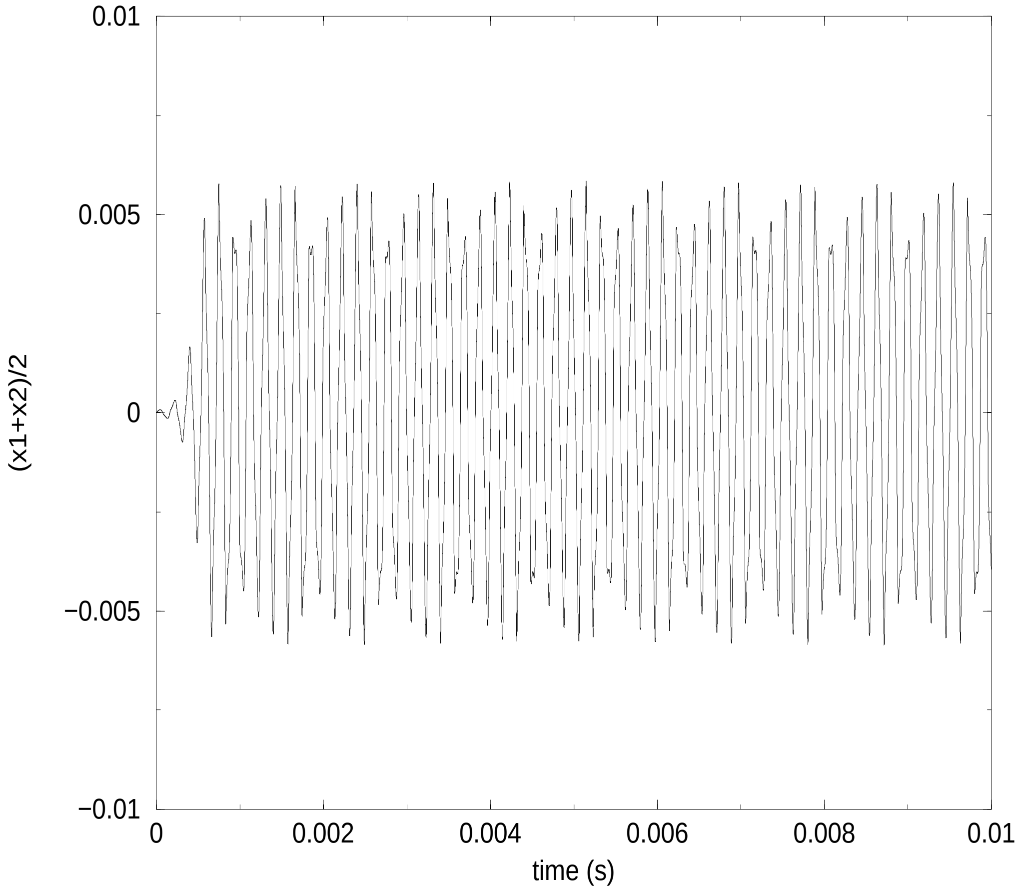

Figure 6: $\bar{X}$ strobed at revolution frequency. $\Upsilon/2 = 1.3$.